Anisotropic behavior of Compacted Decomposed granite soils
다짐화강풍화토의 비등방성 거동특성

안태봉[1] · 함태규[2] · 진한규[3]
Ahn, Tae Bong[1] · Ham, Tae-Gyu[2] · Jin, han-kyu[3]

[1] 우송대학교 공과대학 토목환경공학과 조교수, Assistant Professor, Dept. of Civil and Environmental Engineering, Woosong University
[2] 야무구지대학교 대학원, Graduate Student, Dept. of Civil Engineering, Yamaguchi University
[3] 우송대학교 대학원, Graduate Student, Dept. of Civil and Environmental Engineering, Woosong University

개요(SYNOPSIS) : 다짐화강풍화토의 강도와 변형특성을 조사하기 위하여 불포화배수 삼축압축실험을 실시하였다. 본 실험을 위하여 야마구치현의 시모네세키에서 화강풍화토를 구하였으며 주응력방향과 다짐방향을 0, 45, 90도의 세가지 방향성을 갖도록 하였다. 등방압축시 발생하는 압축변형률은 다짐각도에 따라 크게 영향을 받는다. 이차압축시의 변형거동에 관한 시간의존성은 다짐각도와 관계가 없다. 다짐각도가 압축강도와 변형에 미치는 영향은 특히 낮은 구속압력시에 크다. 다짐각도가 다르다 하더라도 다일러탄시 비율은 다일러턴시로 인한 강도증가와 상관하여 변화한다. 따라서 다짐풍화토는 초기 비등방성 조직을 갖고 있는 모래와 같이 비등방성 역학적 성질을 갖는다고 할 수 있다.

주요어(Key words) : 비등방성, 다짐화강풍화토, 강도, 변형, 다짐방향

1. Introduction

Artificial soil structures, such as riverbanks and embankments, including roads and railways, have a stress history of compaction with their construction. In this process, the compacted soil possesses an anisotropic property. Many laboratory works have been conducted to find the compressibility or mechanical properties of compacted materials. For compacted specimens employed in conventional triaxial tests, the direction of the compaction loading corresponded with the direction of the major principle stress. However, the stress conditions in a soil structure caused by additional loading, such as an earthquake, should varyin terms of the direction of the major principal stress. Therefore, in order to study the detail stability and deformability of astructure using compacted materials, it is necessary to understand the anisotropic properties for the compacted material. Although it has been widely recognized, study of the anisotropicproperty of compacted materials has been limited to clayey soils (Livneh and Komornik, 1967 Onitsuka and Hayashi, 1979). Conversely, saturated clay and soil has been studied by many researchers (Oda et a., 1978;Tatsuoka et al., 1990). Therefore, it is necessary to collect substantial data in order to understand the mechanical properties.

A series of unsaturated-drained triaxial compression tests were performed on compacted materials. Decomposed granite soil was used as this type of material has generally been adopted previously as a construction material. The tests were planned to find not only the degree of anisotropy for the sedimentation angle of the compacted material, but also the influences of the confining stress, degree of saturation and specimen preparation method on the anisotropic properties.

2. Material Properties and Test Methods

2.1 Basic Characteristics

The physical properties of the sample are shown in Table 1, and the grain size distribution curve of the materials in Figure 1.

The quartz, feldspar and colored mineral contents of this sample were about 23, 62 and 15%, respectively. Ignition loss of Toyoura sand, mostly composed of quartz, with a small degree of weathering, 0.4. The ignition loss of the sample was 1.83.

Table 1. Physical properties of the the soil used

Sample	Grain size (mm)	Gs	e_{max}	e_{min}	d_{50}	Ignition loss(%)	Uc	Ip	W_{opt}	ρ_{dmax}
Shimonoseki decomposed granite soil	2	2.685	1.116	0.613	0.555	1.83	7.14	N.P	13.24	1.783

2.2 Sample Preparation

The decomposed granite soil with optimum moisture content(w=13%) was compacted in a container(200 mm×100 mm×200 mm) by hitting with a 2kg rammer. The density of the compacted materials was controlled by the relative compaction, Dc, to be 90%. The degree of compaction was defined as the percentage of the density to the maximum dry density obtained from the compaction test. The rectangular sample was frozen at under -20°C followed by cylindrical triaxial compression of the specimens into a 50mm diameter and 100mm height using a core bit machine, as shown in figure 2. The sample had three different angles of the axial(major principal) direction to the sedimentation plane(compaction plane), 0, 45 and 90 degrees.

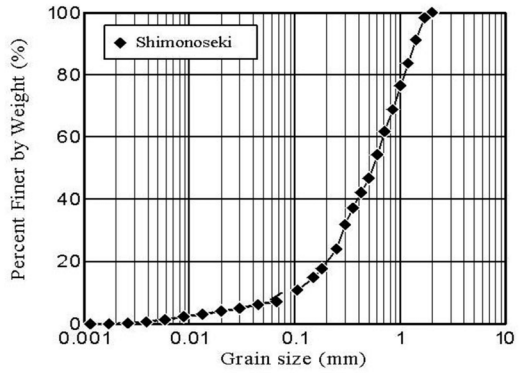

Fig 1. Grain size distribution curve

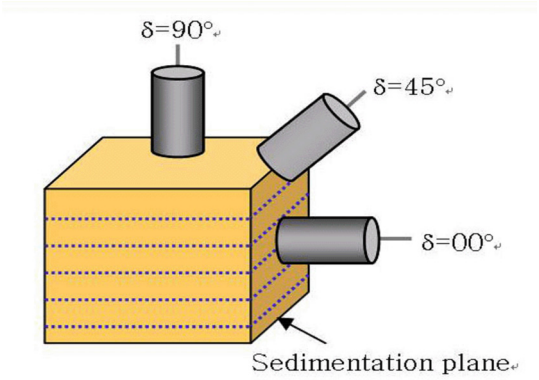

Fig 2. Schematic diagram of the sedimentation angle

2.3 Test

Unsaturated-drained triaxial compression tests were carried out on the specimens at a constant strain rate of 0.1mm/min. A double cell in the apparatus was equipped to measure the volume change of the specimen. The axial strain was measured using the gap sensor of up to 2.0% during the consolidation and initial part of the shear process.

The specimens were set up under a 20kPa confining pressure, with melting for about 6-hours. After this, confining pressures up to, 30, 60, 120 or 240 kPa were applied for times of 1 or 10hours, in order to find the time dependency of the mechanical behaviour of the unsaturated compacted materials.

3. Test results

3.1 Effect of the sedimentation angle on thecompression settel-ment

Figure 3 shows the relationship between the elapsed compression time and the axial strain for a sample subjected to a 60kPa confining stress. There were two compression processes one was the primary compression process, from the beginning to the end of the confining pressure loading, and the other the secondary compression process, after the end of the confining pressure loading. The amounts of axial strain during the primary and secondary compressions were referred to as S_1 and S_2, respectively, as shown in figure 3.

The isotropic compression behavior, S_1, increased suddenly due to the immediate settlement during the primary compression process, after then S_2 showed only a slight non-linear relationship with the function of the logarithm of time during the secondary compression process.

Figure 4 shows the relationship between the axial strain and time under the conditions of 60kPa of confining pressure and 10 hours compressive stress. The arrow in the figure represents the moment the load ended. As δ of the specimen decreased from 90° to 0°, the axial strain S_1 increased.

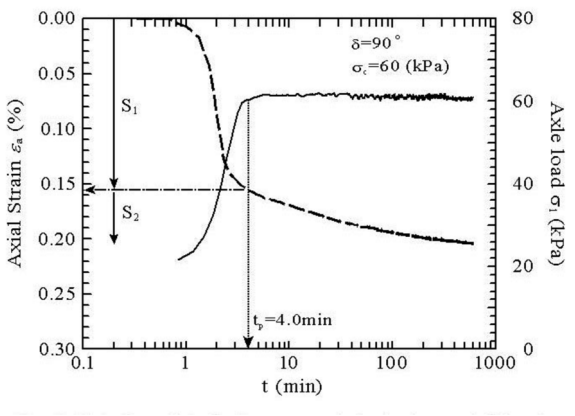

Fig 3. Relationship between axial strain, axial load and compression time

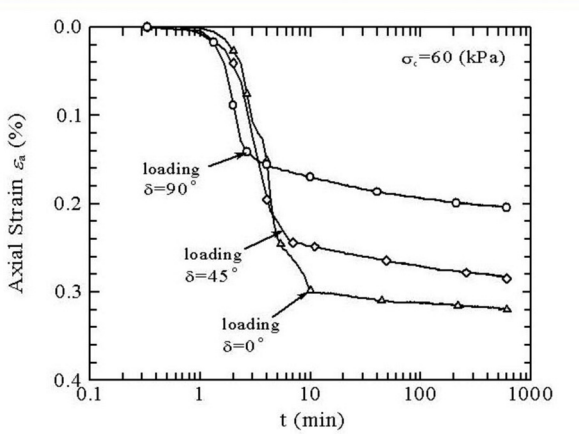

Fig 4. Relationship between axial strain and compression

Figure 5 shows the effect of the confining pressure on the relationship between the axial strain and the duration of compressive stress for samples subjected to 30, 60, 120, 240kPa confining pressures for specimens with δ=90°. As the confining stress increased, the amount of axial strain S_1 also increased. The arrows in the figure represent the moment the load ended. Then, the amount of axial strain, S_2, was approximately the same for all confining stresses. The behaviour of deformation during the secondary compression process was verified as not having any dependency on the confining stress.

Figure 6 demonstrates the relationship between the duration and axial strain in the secondary compression process from figure 4. From figure 6, with longer duration, the rate of decrease became gentler. In addition, the behavior of deformation during the secondary compression process

was dependent of δ. The influence of the sedimentation angle did not appear in the secondary compression process. S_2 was considered to be related to the particle rearrangement and decrease suction factors due to the compression.

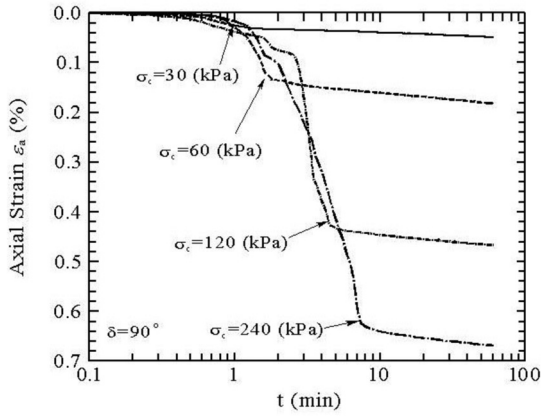

Fig 5. Relation between axial strain and compression

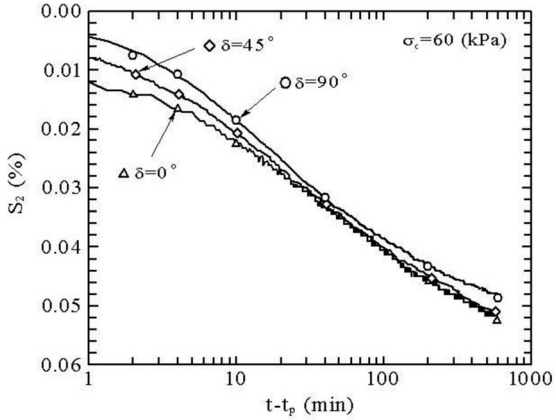

Fig 6. Relationship between S2 and t-tp

3.2 Effect of the sedimentation angle on the strength

In order to investigate the shear property of the compacted specimen with 90, 45 and 0 degree sedimentation angles, drained triaxial compression tests were performed. The deviator stress-axial strain and axial-volumetric strains diagrams for the specimen compressed at 120kPa are shown in figure 7. The deviator stress was defined by $q=(\sigma_1-\sigma_3)$.

In this result for the stress-strain relation, the deviator stress showed a clear maximum stress points, which then slowly deceased. As the value of δ increased from 0° to 90°, the maximum value of the deviator stress qmax also increased, but the axial strain at qmax decreased. In addition, the dilatancy rate at the point of failure increased with increasing δ. Figure 8 shows the change in the deviator stress obtained for strains upto 0.05 % for the specimens the same relation as shown in figure 7.

If the strain behavior changed from a linear to a non-linear deformation, the initial tangent modulus(Etan) is not the same as the Secant Young's modulus(Esec).In this paper, it was assumed that the axial strain at Etan=Esec was the critical condition of elastic deformation. Generally, the Etan of soil materials of no cementation are the same as Esec at approximately less than 0.001% axial strain (Tatsuoka and Shibuya, 1992). The Secant Young's modulus(Esec) was then investigated for the condition of less than 0.001% axial strain on the compacted material.

Figure 9 shows the relation between the Secant Young's modulus at 0.001% strain and the mean principal stress, p. The modulus increased to a linear relationship, having a slope of 0.519. Comparing the dependency for general soil(soil materials of no cementation), which is known to be 0.5 (for example, Hardin and Richart, 1963; Hardin and Black. 1969), the compacted material was found to have approximately the same dependency.

In addition, the δ had no influence on the dependency of Secant Young's modulus on p. Tatsuoka(1990) and Kohata(1995) reported similar results for sand. Therefore, the compacted soil also showed a small strain level(elastic deformation), which was not enough to affect the sedimentation angle. The Secant Young's modulus would only be related to the rigidity of a particle.

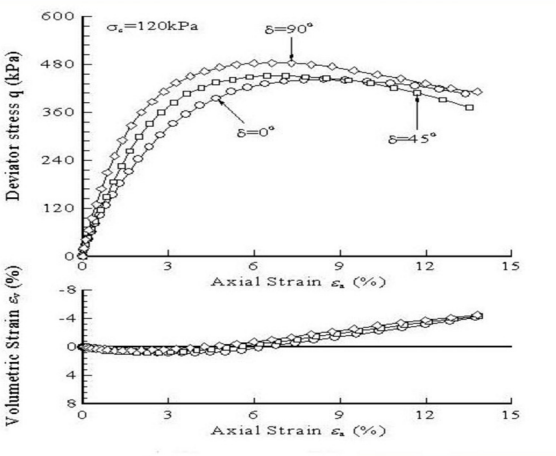

Fig 7. Stress-Strain Relations

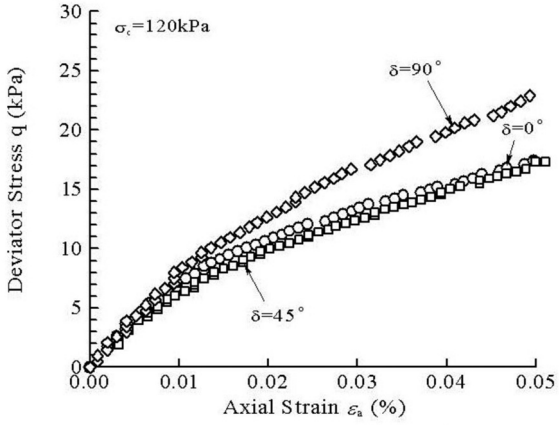

Fig 8. Stress-Strain Relations(ε_a=0.05%)

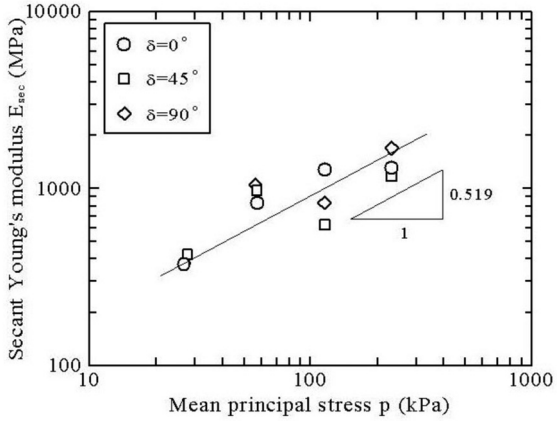

Fig 9. Relationship between Secant Young's modulus and Mean principal stress

Figure 10 shows the relationship between the secant shear resistance angle at peak shear stress (ϕpeak) and δ. The angle ϕ was calculated by the following equation.

$$\phi = \sin^{-1}\frac{(\sigma_1 - \sigma_3)}{(\sigma_1 + \sigma_3)} \qquad (1)$$

where σ_1 is the major principal stress and σ_3 is the minor principal stress.

As the value of δ increased from 0° to 90° the angle(ϕpeak) also increased. The angle (ϕpeak) of the 10-hours compressed specimens appeared to be approximately 2 degrees lower than that of the 1-hour compressed specimens. The degrees of saturation of the 1-hour and 10-hour compressed specimens were approximately 60% and 65%, respectively. Thus, the decrease in the strength over 10 hours would be related to the increase in saturation of the specimen, which also caused the decrease in suction.

In figure 10, the strength data on Ube decomposed granite soils prepared by the air pluviation method has been indicated(Nakata et al, 1998). The angle(ϕpeak) of Ube appeared to be approximately 10 to 15 degrees lower than that of Shimonoseki. On the basis of this comparison, the influences of the sedimentation angle appear to be similar, irrespective of the

sample preparation method.

Figure 11 represents the effect of the sedimentation angle shown by Tatsuoka et al.(1990), who proposed the normalization of the shear resistance angle to that of the shear resistance angle 90° δ, ϕ(δ)/ϕ(δ=90°). The data for Toyoura sand, obtained by Oda et al, (1978) and Tatsuoka et al.(1990), are also shown in this figure. All specimens shown in figure 11 appear to have similar tendencies, in that the value of ϕ(δ)/ϕ(δ=90°) increased with increasing δ, although factors relating to the specimens, such as the initial density, the confining stress, the condition of sedimentation and preparation method, were different.

Figure 12 shows the relationship between the secant shear resistance angles at peak shear stress(ϕpeak) and the mean principal stress, p. As the mean principal stress increased, ϕpeak decreased steeply. The slope became steeper as δ became large. The effect of the sedimentation angle on the strength of deformation was clear with low mean principal stress. In the case of Ube, the tendency for a steep slope was shown to be very gentle with increases in the mean principal stress, p, compare with the data of Shimonoseki.

It was thought that the initial fabric arrangement would remain nearly constant in alow confining stress. As the confining stress increased, the particleswere rearranged by particle breakage, such that the effect of the sedimentation angle disappeared under high confining stress.

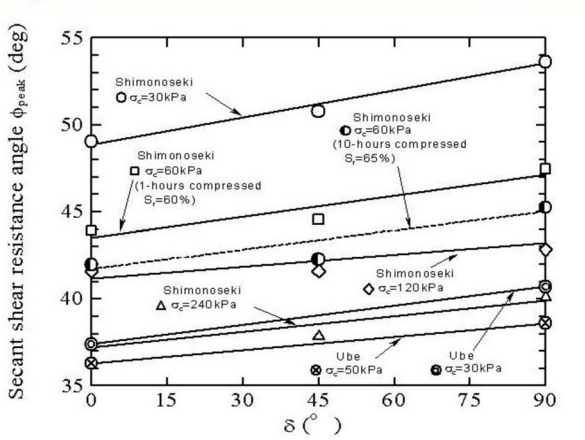

Fig 10. Relationship between secant shear resistance angles at peak shear and δ

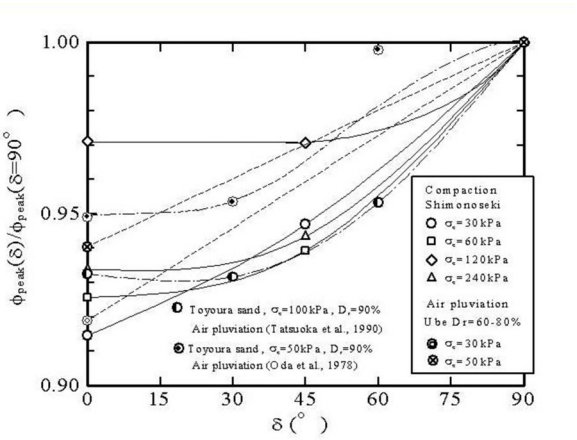

Fig 11. Relationship between ϕ (δ)/ ϕ(δ=90°) and δ

3.3 Effect of the sedimentation angle on the dilatancy

In order to show the effect of the sedimentation angel on the dilatancy, the ratio of the volumetric strain increment to that of the deviator under peak stress conditions, $(-d\varepsilon v/d\gamma)_{peak}$, was examined. Figure 13 shows the ratio of $(-d\varepsilon v/d\gamma)_{peak}$ for an angle of sedimentation $(-d\varepsilon v/d\gamma)_{peak}$ for a δ of 90°. The ratio $(-d\varepsilon v/d\gamma)_{peak}$ /$((-d\varepsilon v/d\gamma)_{peak}$ at δ=90°) was plotted against of δ. So, when d was equal to 90°the ratio became 1. As the confining stress increased, the ratio, $(-d\varepsilon v/d\gamma)_{peak}$ /$((-d\varepsilon v/d\gamma)_{peak}$ at d=90°),decreased. The $(-d\varepsilon v/d\gamma)_{peak}$ /$((-d\varepsilon v/d\gamma)_{peak}$ at δ=90°) with a confining stress of 30kPa was 0.58. As the confining stress increased, the value of $(-d\varepsilon v/d\gamma)_{peak}$ /$((-d\varepsilon v/d\gamma)_{peak}$ at δ=90°) was approximately 1.0.

The compacted decomposed granite soils had lower values of $(-d\varepsilon v/d\gamma)_{peak}$ at δ=0)/$((-d\varepsilon v/d\gamma)_{peak}$ at δ=90°) than the data for the air pluviated decomposed granite and Toyoura sand.

Figure 14 shows the relationship between (ϕpeak-ϕcv)/(ϕpeak-ϕcv at δ=90°) and δ, where ϕcv is

the shear resistance angle at the constant volume condition and ϕpeak-ϕcv is considered the increment part of the strength due to dilatancy of the specimen. The value of ϕcv was defined as the minimum value in all tests of the mobilized angle where the deviator strain reached 14%. As the confining stress increased and the value of δ decreased, the value of ϕpeak-ϕcv became smaller. Moreover, the tendency for the effect of the sedimentation angle at strength, as shown in figure 14, agreed with the tendency of the effect of the sedimentation angle on the dilatancy, as shown in Figure 13.

Figure 15 shows the relationship between the increment of strength due to dilatancy, ϕpeak-ϕcv, and the dilatancy rate, $(d\varepsilon v/d\gamma)_{peak}$ at failure. As $(d\varepsilon v/d\gamma)_{peak}$ increased, ϕpeak-ϕcv, also increased. The same tendency was obtained for all specimen used in this paper. It was also recognized that although the sedimentation angle and preparation methods were different, the dilatancy rate at failure was related to the increment of strength due to dilatancy. Therefore, it can be concluded that the difference between the peak strength ϕpeak and the residual strength ϕcv was dominated by the dilatancy for compacted specimens, as with sand.

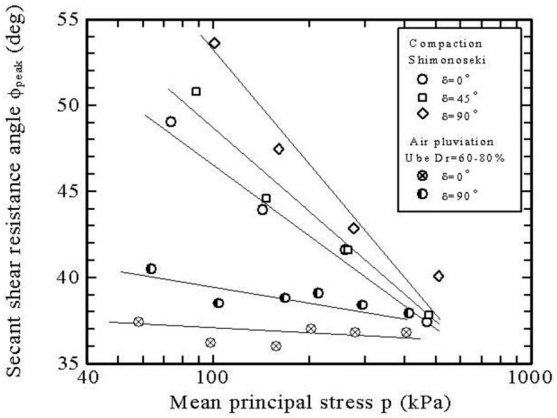

Fig 12. Relationship between secant shear resistance angles at peak shear and mean principal stress

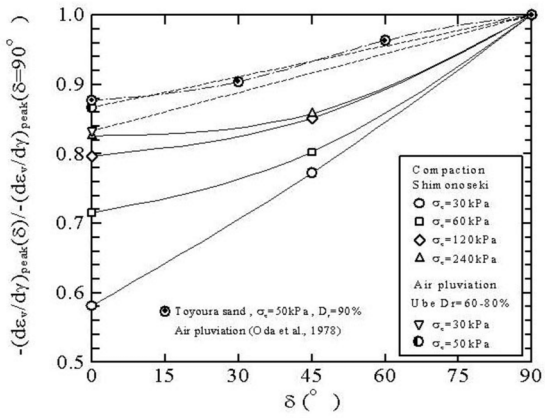

Fig 13. $-(d\varepsilon_v/d_\gamma)_{peak}(\delta)$ /$-(d\varepsilon_v/d_\gamma)_{peak}(\delta=90°)$ and δ Relations

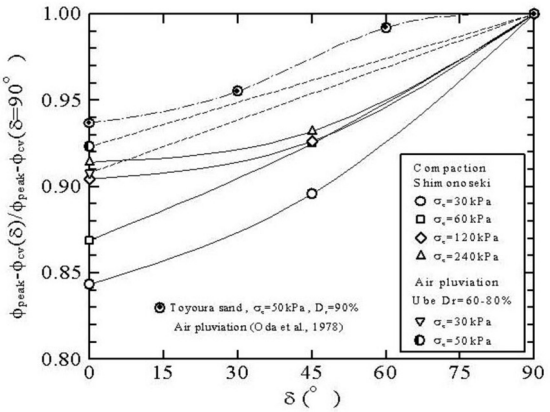

Fig 14. $\phi_{peak}-\phi_{cv}$ (δ)/ $\phi_{peak}-\phi_{cv}$ (at δ=90°) and δ Relations

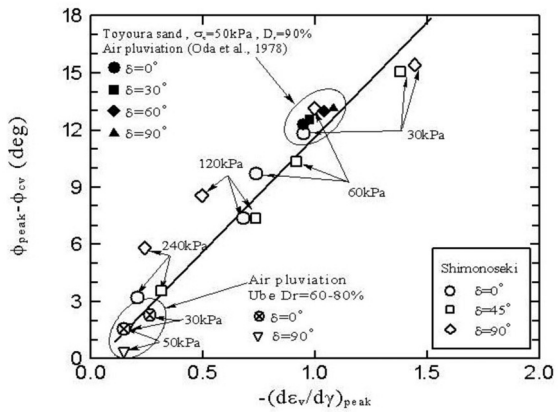

Fig 15. Relationship between $(\phi_{peak}-\phi_{cv})$ and $-(d\varepsilon v/d\gamma)$

3.4 Discussion on initial fabric of compacted material

Lambe(1958) started a way of thinking about the structure of compacted soil, and although many

researchers have tried to examine the fabric(structure) of compacted soil (Seed, Mitchell, and Chan, 1960) no consensus has been completely established. Attempts to observe the fabric arrangement of the specimens used in this paper using microscopy were made, but the fabric anisotropy could notbe confirmed. Generally, the fabric anisotropy of saturated sand due to air-pluviation sedimentation has been known to develop in the direction of sedimentation.

Onitsuka and Hayashi(1979) pointed out that the strength anisotropy of compacted sandy soils was caused by the direction of fabric arrangement, as the direction of the fabric arrangement was willing to orientate perpendicularly to the compaction direction.

From the result of the unsaturated-drained triaxial compression tests on the compacted decomposed granite soils in this paper, it can be concluded that the compacted specimen had anisotropic mechanical properties the same as those initially found with sand. It would be meaningful to take the anisotropy properties into account for a performance based design of a compacted soil structure to an external force, such as a large earthquake.

4. Conclusions

A series of unsaturated-drained triaxial compression tests were performed on compacted materials. The tests were planned to find the effect of, not only the degree of anisotropy for sedimentation angle of compacted material, but also the influence of confining stress, saturation degree and specimen preparation method on the anisotropic properties. The following conclusions can be drawn from this study:

(1) The compression strains of specimens were strongly influenced by the sedimentation angle.
(2) The Secant Young's modulus showed the same behaviour for all specimens, even with different δ.
(3) The effects of the sedimentation angle on the triaxial compression strength and deformation were clear with a low confining stress.
(4) Although the sedimentation angle and preparation methods were different, the dilatancy rate was related to the increments in strength due to dilatancy.
(5) The compacted specimen can be considered to have anisotropic mechanical properties, the same as the initial fabric anisotropy of sand.

References

1. Hardin, B.O. and Richart, F. E.Jr. 1963. Elastic wave velocities in granular soils, *Journal of SMF Div., ASCE,* Vol. 89, No. SM1: 3365.
2. Hardin, B.O. and Black, W. L. 1969. Vibration modulus of normally consolidated clay, *Journal of the SMF Div., Proc. ASCE,* Vol. 95, No. SM6: 15311537.
3. Kohata, 1995. Inherent and induced anisotropy of sedimentary softrock, *Proc. Of 10ARC*: 3336.
4. Livneh, M., Komornik, A. 1967. Anisotropic strength of compacted clay, *Proc., 3rd ASIAN Reg. Conf. On SMFE*, Vol.1: 298304.
5. Lambe, T. W. 1958. The structure of compacted clay, *Proc., ASCE.,* Vol 84, SM2: 16551165535.
6. Nakata, Y., Hyodo, M. and Murata, H 1998. Single particle crushing and mechanical behaviour of decomposed granite soil, *Proceedings of the international symposium on problematic soils., IS-TOHOKU'98. SENDAI, JAPA*:497483.
7. Oda, M. 1981. Anisotropicstrength of cohesionless sands, *Jour of Geotechnical Eng. Div., Proc. Of ASCE*, Vol.107, No. GT9: 12191231.

8. Oda, M., Koishikawa, I., and Higuchi, T. 1978. Experimental study of anisotropic shear strength of sand by plane strain test, *Soils and Foundation*, Vol. 18, No.1: 2538.
9. Onitsuka, K., Hayashi, S., 1979. Studies on compression and strength Anisotropy of compacted soils, *in Japanese. JSCE.* Vol.19, No.3, Sept: 113123.
10. Seed, H.B., Mitchell, J.K. and Chan, C.K. 1960. The strength of compacted cohesive soils, *ASCE., Research Conf. On the Shear Strength of Cohesive Soil, Boulder,* Colorado: 169273.
11. Shibuya, S., Mitachi, T., Fukuda, F. and Degoshi, T. 1995. Strain rate effects on shear modulus and damping of normally consolidated clay, *Geotechnical Testing Journal,* Vol. 18, No. 3: 365375.
12. Tatsuoka, F., Nakamura, S., Huang, C. and Tani, K. 1990. Strength snisotropy and shear band direction, *Soils and Foundation*, Vol. 30, No.1: 3554.
13. Tatsuoka, F., Shibuya, S. 1992. Deformation characteristics of soils and rocks from field and laboratory tests, *Keynote Lecture, Proc. Of 9th Asian Regional Conf. On SMFE,* Vol. 2: 101170.
14. Tatsuoka, F, 1994. Stiffness of hard soils and soft rocks in engineering applications, *Pre-failure deformation of geomaterials*, Vol. 2: 9471063.
15. Yong, R.N., Warkentin, B.P. 1966. Introduction to Soils Behavior: 106107.